American Scientific Research Journal for Engineering, Technology, and Sciences (ASRJETS)
ISSN (Print) 2313-4410, ISSN (Online) 2313-4402

http://asrjetsjournal.org/

Three-Dimensional Verification Model of Floating Wind Energy Converter Using LS-DYNA3D Code

Mohamed Abdalla Almheriegh*

Assistant Professor, Department of civil Engineering, Faculty of Engineering - Tripoli University, P O Box 82677, Tripoli, Libya
Email: malmherigh@gmail.com

Abstract

The use of an explicit LS-DYNA3D code for analysing full-scale structure requires validation using robust methodology and formulations. A characteristic prototype three-dimensional model of a floating object been developed to further test the action and available features in the code before they employed in three dimensions full-scale model. In an attempt to increase confidence in the expected findings, before to expand to the full-scale floating turbine to be analysed by this code. Employed features such as; different material cards, contact, property cards, control cards, constraints and boundaries are all checked and have shown good agreement with hand calculation and or energy dissipation and engineering judgement.

Keywords: verification of floating wind converter analysis; 3-D analysis of floating wind energy turbine; modeling of floating wind energy turbine by LS-DYNA3D code; 3-D floating wind converter for LS-DYNA3D code modeling; dynamic analysis of structure.

1. Introduction

Features available in LS-DYNA3D explicit code such as the 'ALE' (Arbitrary Lagrangian Eulerian) is been used for many fluid-structure interaction problems, mainly for transient impact analyses where severe mesh deformation of the Lagrangian material presents a problem. To date though there appears to be little information specifically on modelling buoyancy effects and subsequent dynamics. Although we are not expecting the mesh to deform in this case, it could provide the appropriate buoyancy and sought fluid material effects. This could however be at the expense of increased elements and solution runtime, so model complexity has monitored carefully.

---

* Corresponding author.

Typically, if using 'ALE', the turbine will have to float in a fluid 'half-space' of a size, which will best represent the effects of the pseudo-infinite sea. The boundaries will need careful consideration, and perhaps employ non-reflecting (energy absorbing) representation. It is this representation, which employed in this work, and a study of buoyancy conducted for verification purposes. Due to the time and resources devoted to the design of a floating wind energy converter, a detailed investigation required via 2-D modelling as well as 3-D modelling in order to build confidence in design. While 2-D model already published and showed good results, the purpose of this work is to build more confidence in the design through 3-D characteristic model for further investigation.

2. Three-dimensional stick model

In order to build an explicit finite element model of a floating wind energy converter Figure 1. First modelling a stick of (0.1m x 0.1m) square cross section and 0.4m height Figure 2. Stick is positioned vertically in side cube of ALE water elements 'in blue' to model water quanta of (1.1m x 1.1m x 0.6m) Figure 3. Atop it another ALE air elements of (1.1m x 1.1m x 0.2m) Figure 4. All mentioned dimensions are in the x, y and z directions respectively. The density of the floating stick is determined according to the buoyancy principle.

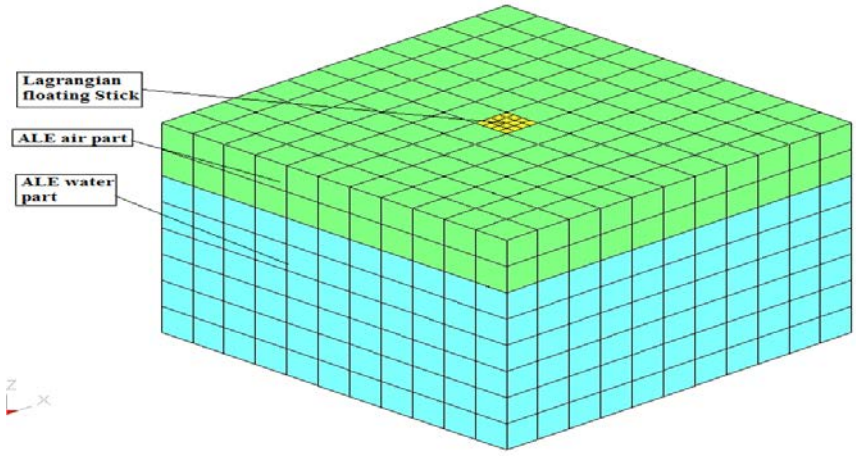

Figure 1: The 3-D Stick model in air and fluid media

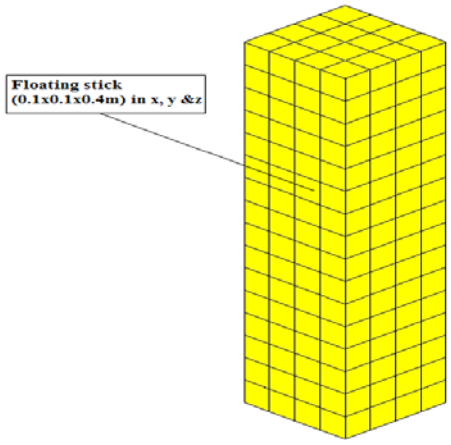

Figure 2: 3-D floating stick

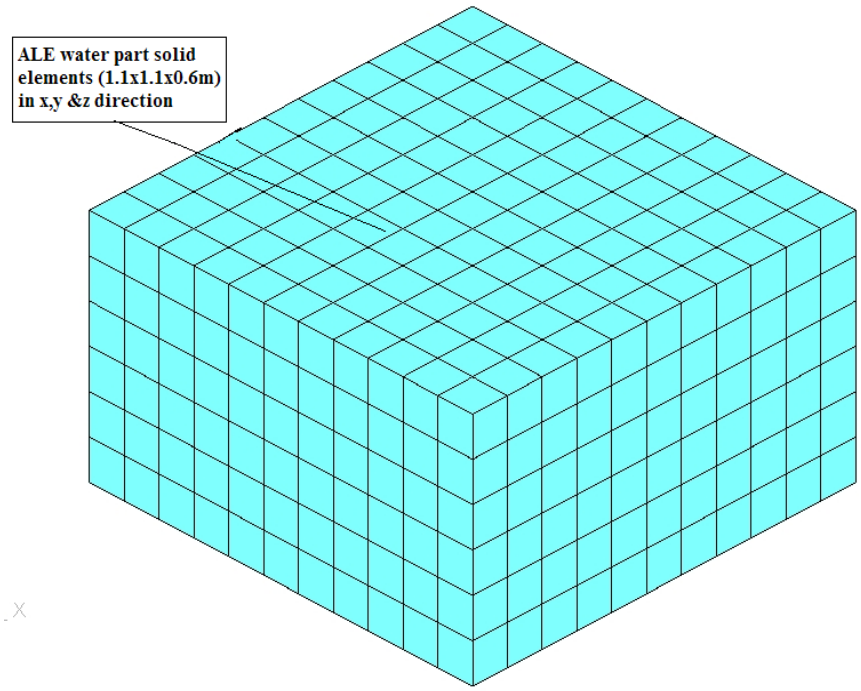

Figure 3: 3-D Water part

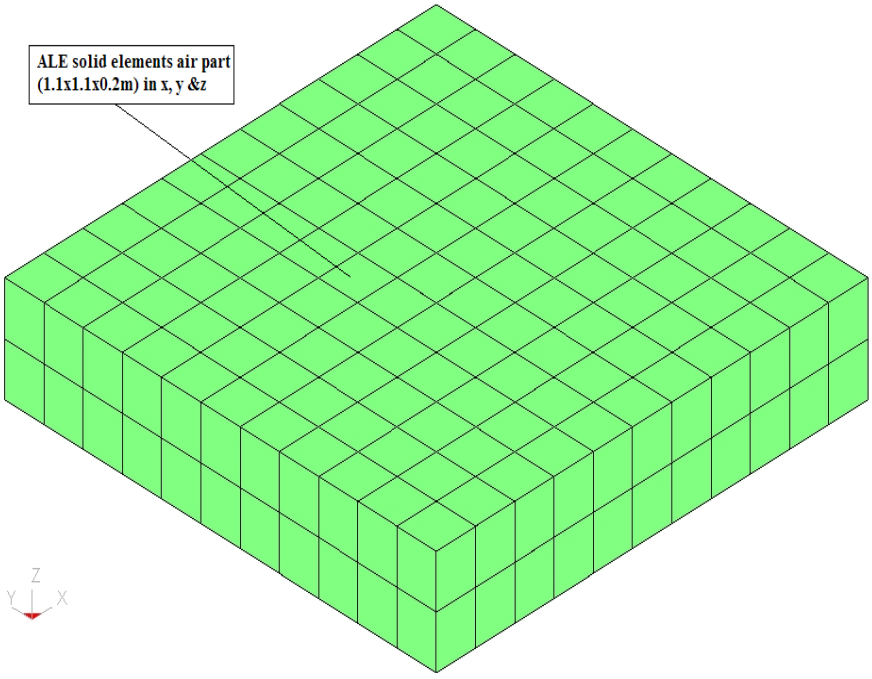

Figure 4: 3-D Air part

The displaced volume = 0.1 x 0.1 x 0.2 = 0.002 m^3 and uplift buoyancy force is

$F_{buoyancy}$ = 0.002 x 1025 x 9.81 = 20.11 N, this is close enough to the z-force shown in Figure 5.

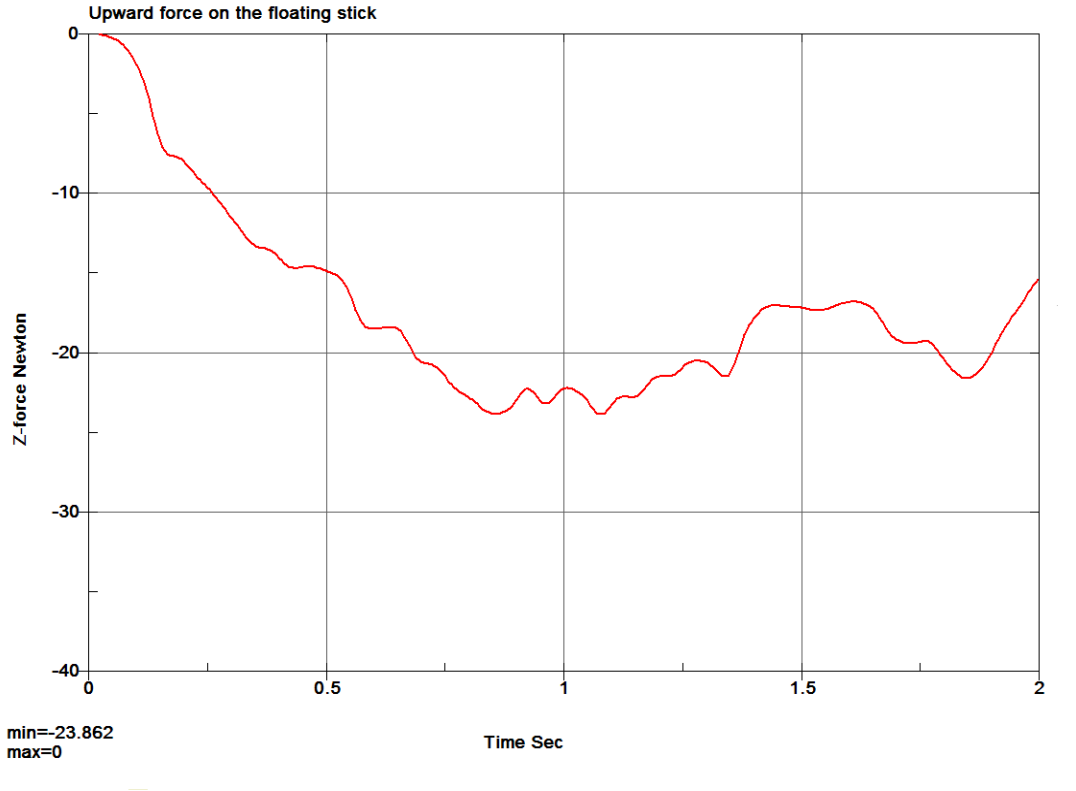

Figure 5: Uplift buoyancy force on the floating stick bottom

Meanwhile the z-direction stress under the floating stick been calculated as follows:

$\sigma_{zz} = \frac{20.11}{0.1 \times 0.1} = 2011$ Pa, this value is close enough to the calculated value shown in Figure 6.

Moreover, for base side element of the floating stick, the water pressure due to vertical position of this element centre at 0.1875m elevation is:

P_{xx} = 0.1875x1025x9.81 = 1885.36 Pa this in close agreement with the calculated pressure value for the same element shown in Figure 7.

In the same sequence picking up an element at the edge of the stick base, the forces calculated at the two edge nodes of the element is (-1.6 N) while those at the top edge of the same element is (-3.2 N) as calculated by the code.

Therefore, this element share of these forces is (-2 x 1.6/2 + (-3.2) x 2/4) = -3.2 N this is translated to an element stress in x-direction = $\frac{-3.2}{(0.025) \times (0.025)}$ = -5120 Pa which is close to the value shown in Figure 8.

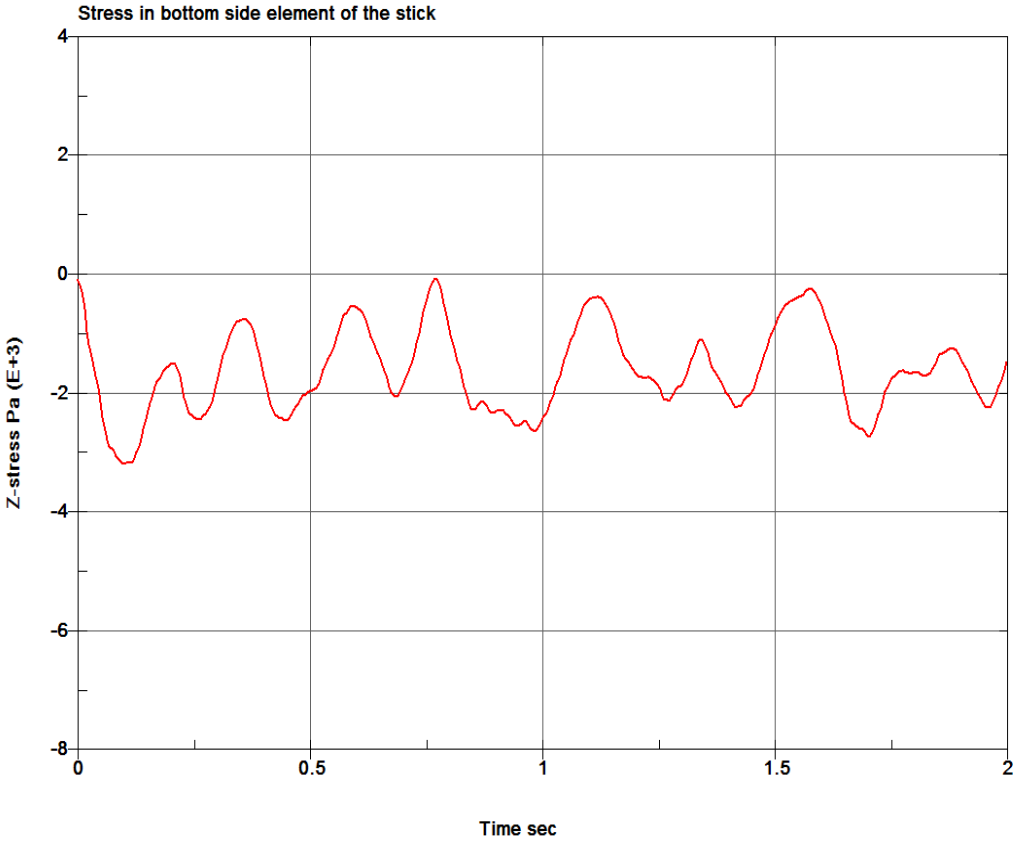

Figure 6: Bottom face stress of the floating stick

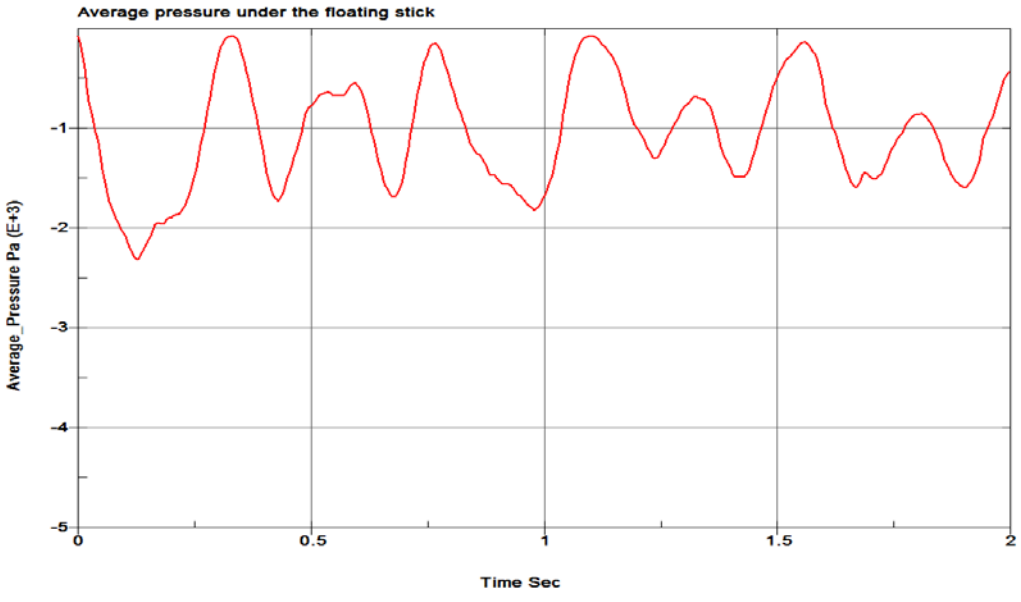

Figure 7: Bottom face pressure on the floating stick

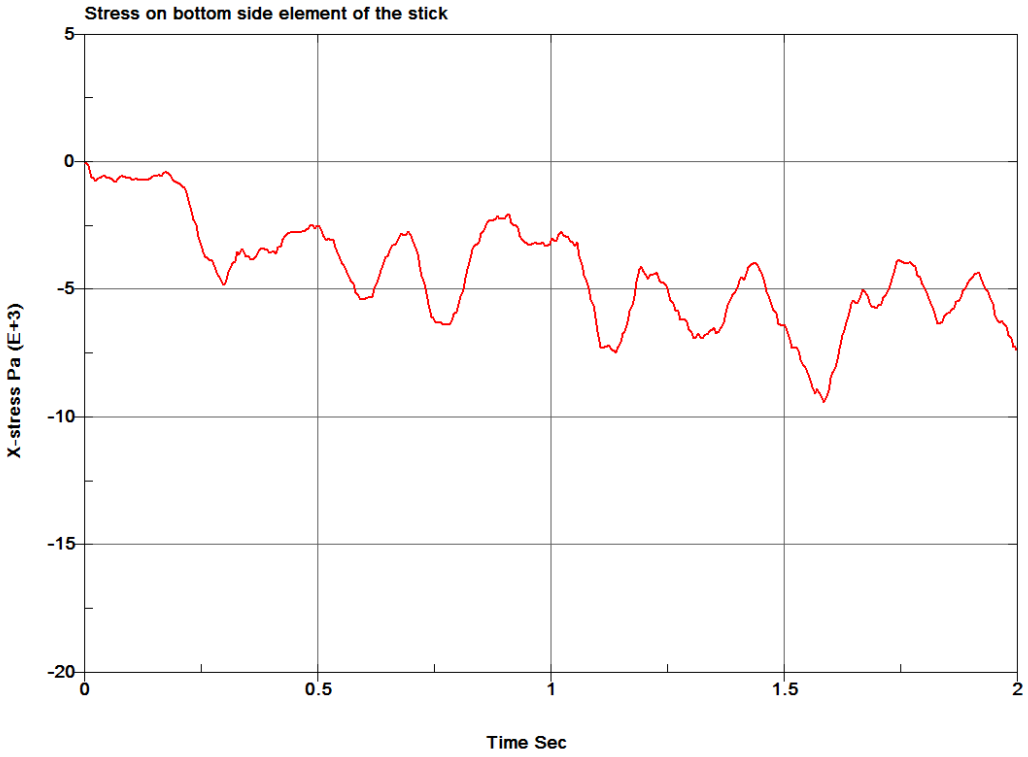

Figure 8: Stress in the base side element of the stick

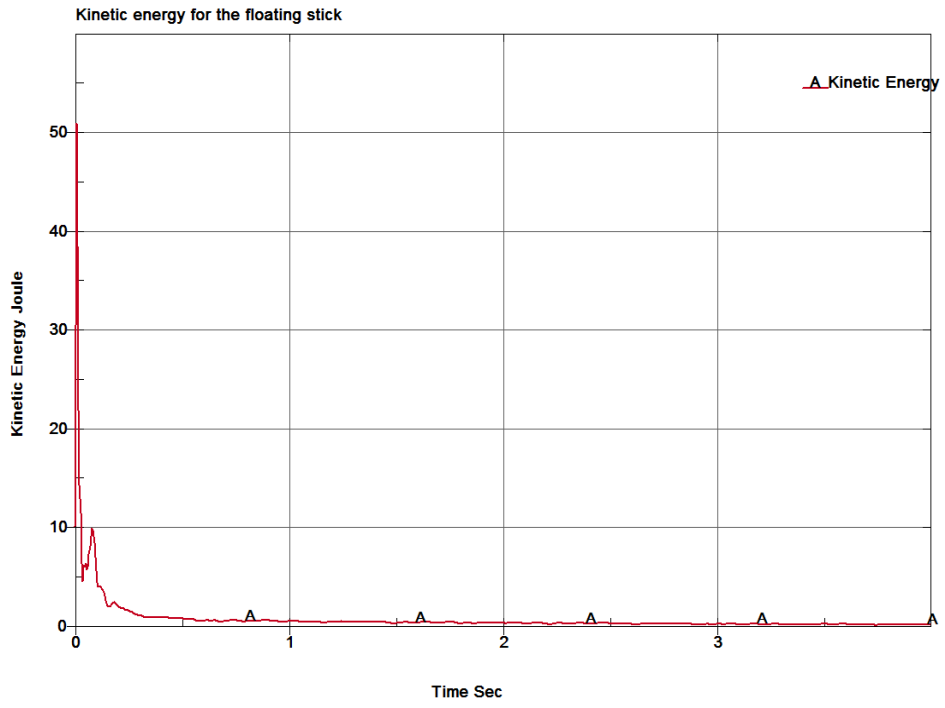

Figure 9: Kinetic energy for floating stick model

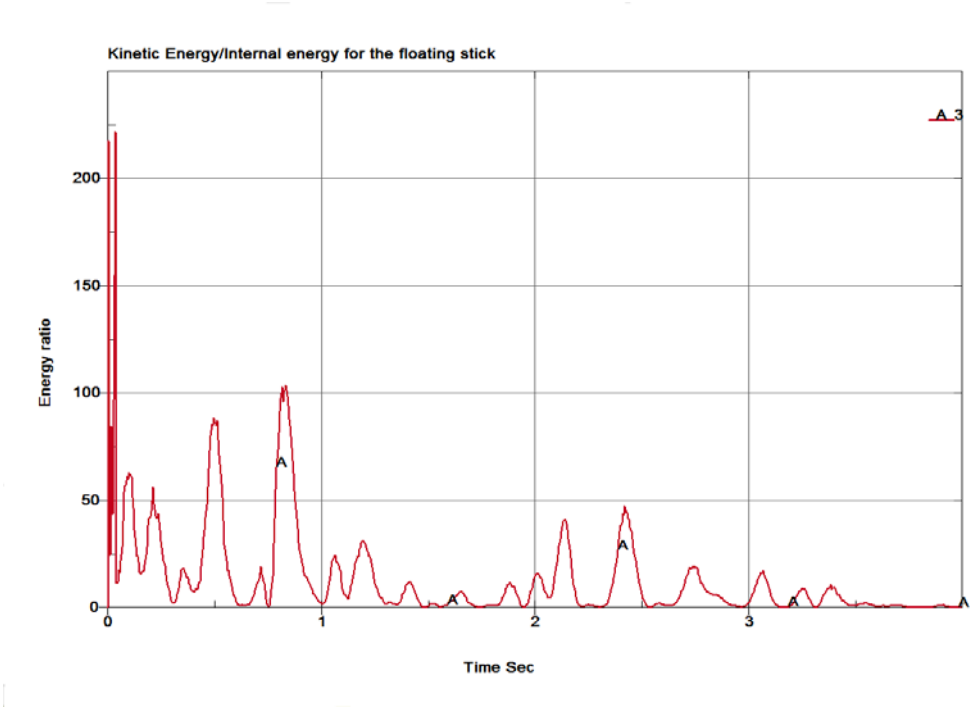

Figure 10: Energy ratio for the floating stick model

The system kinetic energy and energy ratio shown in Figure 9 and Figure 10 shown to be well within the converged stable system with nearly unity for energy ratio and failing to zero kinetic energy.

3. Characteristic Model

Building on the previous findings; Mohamed [1], and based on the concept of the floating wind turbine Vugts J. h. and his colleagues [2], Henderson A. R. and his colleagues [3], characteristic model is developed and analysed to further confidence in the expected findings. The model Figure 11, Figure 12 typically consisting of the mean parts forming the structure of the full detailed model. The different parts summarized below:

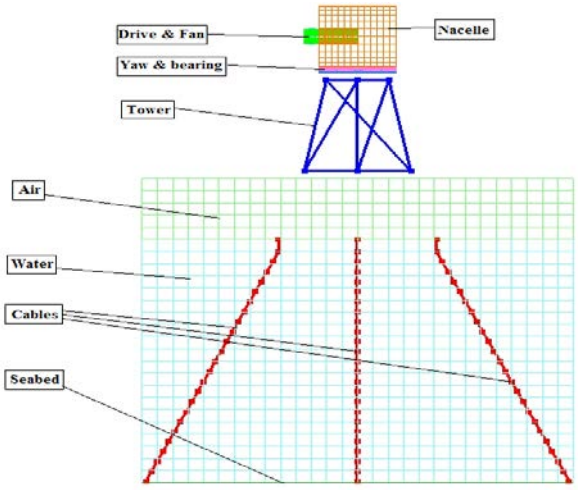

Figure 11: Characteristic model of the floating wind turbine

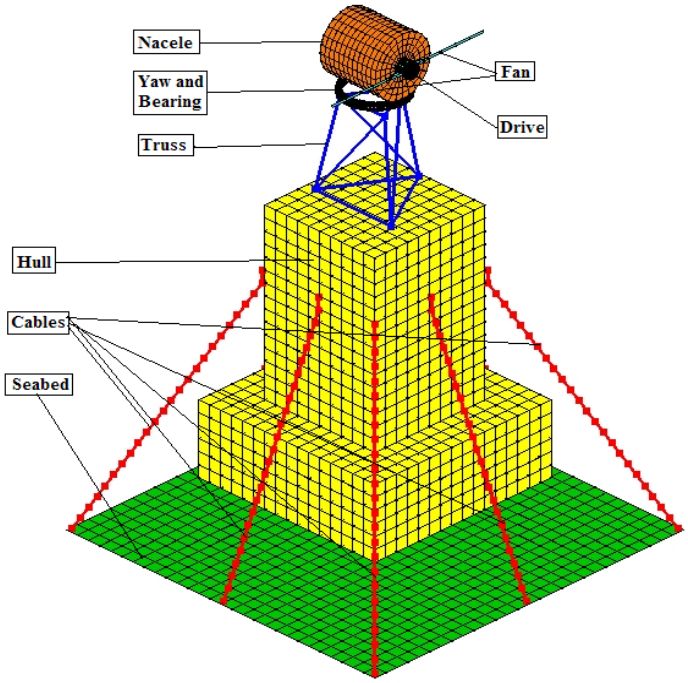

Figure 12: Characteristic model excluding ALE parts

3.1 Water Part of the Characteristic Model

This is an (ALE) solid brick elements simulating the hosting liquid media as shown in Figure 11 and Figure 13 it is a cube of dimensions (1.12mx1.12mx0.8m) bound from underneath by the seabed shell part and from top by the air part. As for the boundary conditions the side nodes of the ALE mesh are restrained against movement to help building pressure within the elements body while the side segments of the outer elements are defined as non-reflecting boundary surface to simulate the infinite medium through the offset of the reflected wave action. The Grüneisen equation of state used for pressure generation within this part.

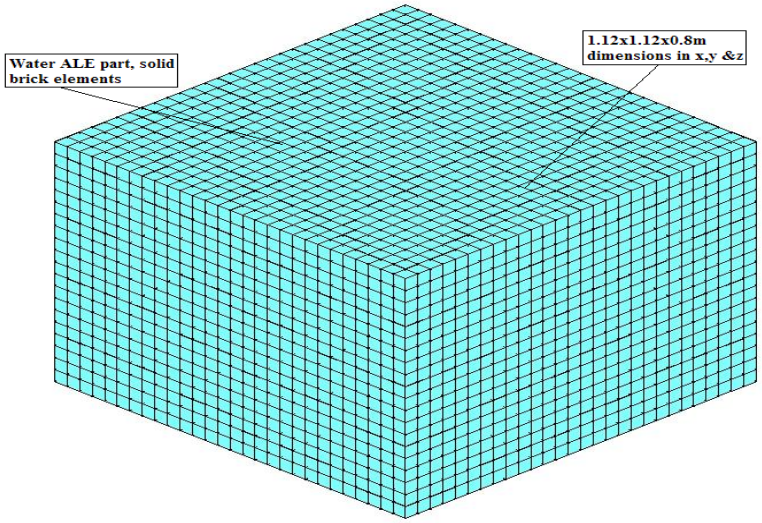

Figure 13: Water (ALE) part of the characteristic model

3.2 Air Part of the Characteristic Model

This is the second ALE part simulating air fluid part atop the water part, shown in Figure 11 and Figure 14 it is consisting of solid brick elements of dimensions (1.12mx1.12mx0.2m). Pressure within air elements initiated using polynomial equation of state and coincident nodes between ALE parts are merged simulating proper contact.

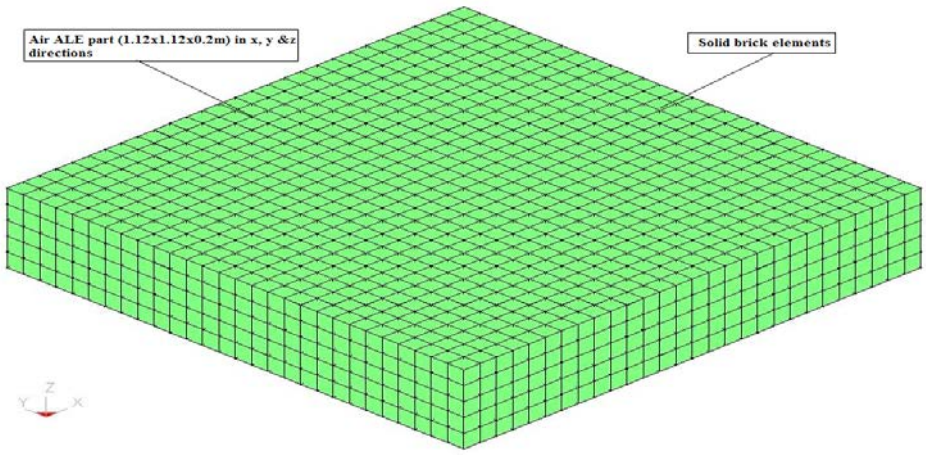

Figure 14: Air (ALE) part of the characteristic model

3.3 Cable Part of the Characteristic Model

This is taut polyester cables and as shown in Figure 11, Figure 12, Figure 15 a and Figure 15 b the 8 cables are of total length 7.24m pined at top ends to the floating support and at the bottom ends to the seabed part. More than one node of the meeting parts are constrained against translation to the cable end nodes, thus avoiding high stress concentration and forcing the failure (if any) to occur in cables. The LS-DYNA3D cable material (type 71) used to model this part. Cables coupled to water using constrained Lagrange in solid keyword.

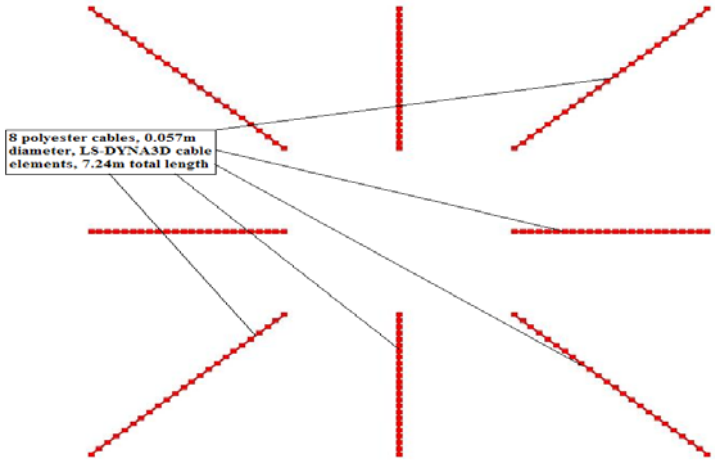

Figure 15 a: Cable part of the characteristic model (plan view)

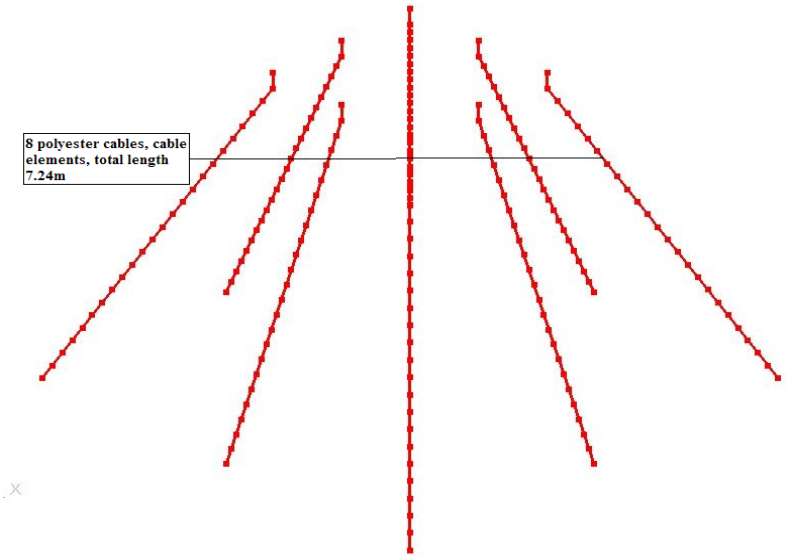

Figure 15 b: Cable part of the characteristic model (isometric view)

3.4 Floating Support Part of the Characteristic Model

Typically made of solid brick elements to model the buoyant support and of the shown dimensions of which 0.60m submerged in water while the above section is hollow to lower the centroid of the hull, thus assessing stability. The action of submergence modelled in LS-DYNA3D using initial volume function to define the space occupied by the hull in ALE parts. Coupling between this part and ALE parts had done using constrained Lagrange in solid keyword. The buoy shown in Figure 11, Figure 12 and Figure 16. The used density of this part is determined according to the buoyancy principle. Concrete mechanical properties assumed.

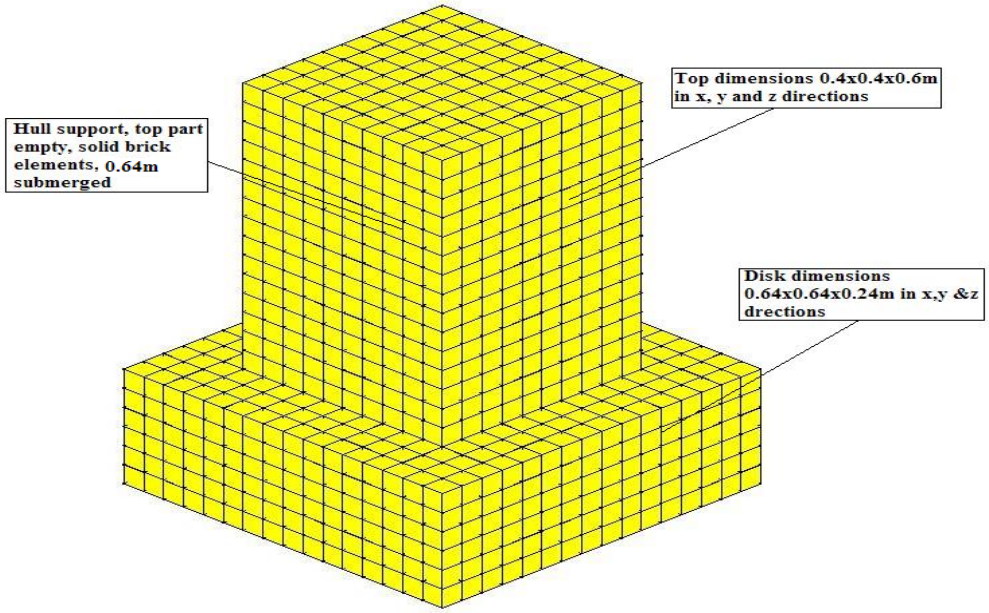

Figure 16: Floating support of the characteristic model

3.5 Tripod Truss Part of the Characteristic Model

As shown in Figure 11, Figure 12, Figure 17 and Figure 18, the tripod truss is made of hollow steel

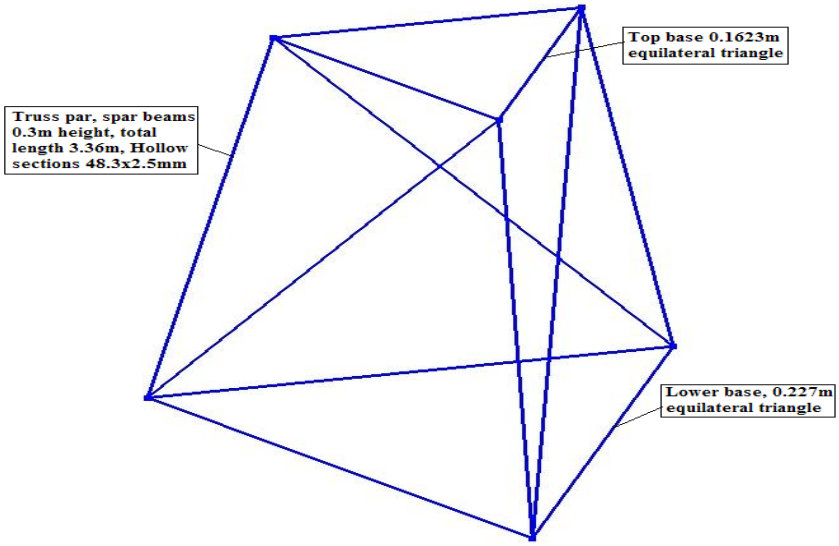

Figure 17: Tripod truss of the characteristic model

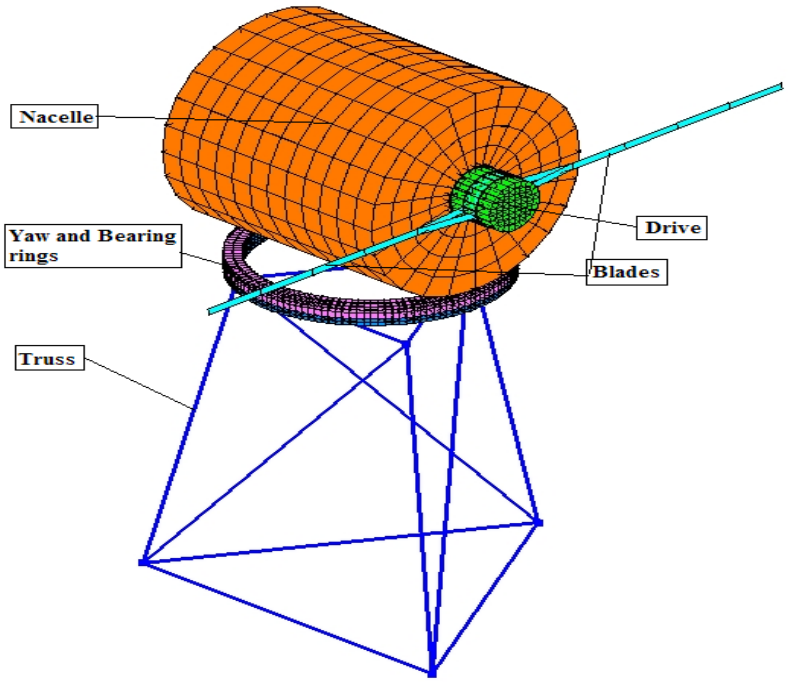

Figure 18: Parts above float of the characteristic model

sections (48.3x2.5mm), having a total elements length of 3.9m, the truss is of 0.4m height and modelled using truss beam elements. Its function is to mount other parts to the required level.

3.6 Bearing Part of the Characteristic Model

The bearing is the part offering the rotational movement of the yaw system firmly fixed to the tower top and fixed to the parts above it through rotational free 'joint revolute' in order to simulate this action the bearing part is split to two parts; namely the bearing part and the yaw part. Both parts are defined as rigid material giving enough confidence in their stiffness and paving the way for the use of the 'revolute joint' restraint as required by the code. Shown in Figure 11, Figure 12, Figure 18 and Figure 19 the bearing part made of solid brick elements and of geometry (0.2m, 0.175m, 0.0125m and 0.006m defining external diameter, internal diameter, height and thickness respectively). Bearing part connected to truss part by merging truss nodes as extra nodes to bearing part (rigid part). Steel mechanical properties used for this part.

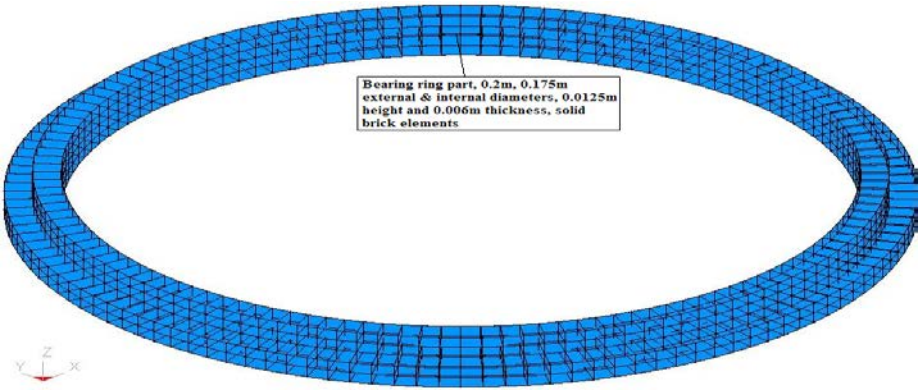

Figure 19: Bering part of the characteristic model

The yaw ring is modelled using solid brick elements of dimensions (0.2m, 0.175m, 0.0125m and 0.006m defining external diameter, internal diameter, height and thickness respectively). As shown in Figure 11, Figure 12, Figure 18 and Figure 20. Yaw part firmly connected to nacelle above it by merging the two rigid parts. Steel mechanical properties used for this part.

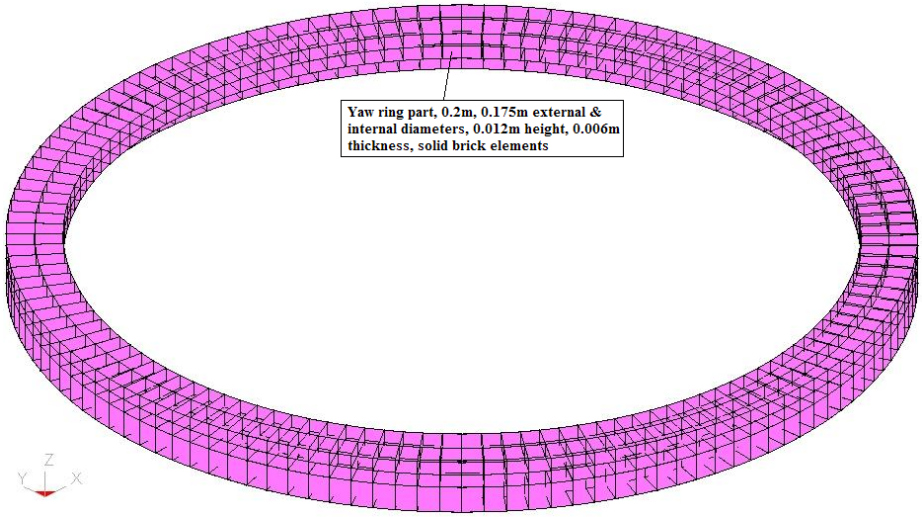

Figure 20: Yaw part of the characteristic model

3.7 Nacelle Part of the Characteristic Model

As explained earlier, it is the housing space for electricity generation equipment, connected to both the yaw through rigid body merge and to the rotor parts via 'joint revolute' both connections intended to give rotational free but rigid connections thus requiring the nacelle be defined as rigid material. Fully integrated shell elements (type 16) used for this part to avoid hourglass energy effects, and structural steel mechanical properties assumed. The nacelle geometry is 0.2m length and 0.2m diameter for external surface while for the internal cylinder it 0.1m length and 0.05m diameter. Nacelle geometry and arrangement in the assembly shown in Figure 11, Figure 12, Figure 18 and Figure 21.

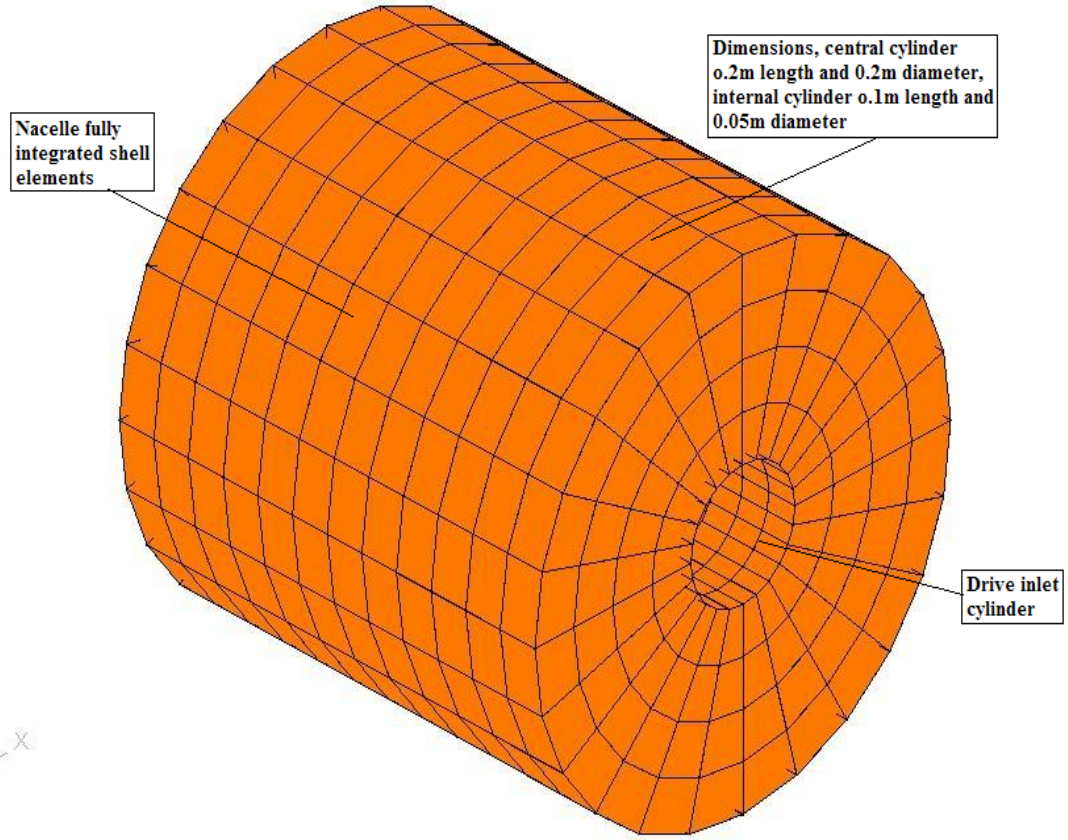

Figure 21: Nacelle part of the characteristic model

3.8 Rotor Parts of the Characteristic Model

This is typically would have consisted of three parts; here two parts only are used for the purpose of this verification. First the drive part: solid shaft of o.14m length and 0.05m diameter modelled with rigid material (joint requirement) and solid brick elements. Second the blades part: this is modelled in 2 blades of 0.6m diameter modelled by fully integrated shells assuming 'GRP' mechanical properties, all nodes of the blades are constrained to drive (rigid part) as extra nodes thus assuring full fixity and integral rotation. The drive part geometry and location in the assembly shown in Figure 11, Figure 12, Figure 18 and Figure 22. While that of the blades part shown in Figure 11, Figure 12, Figure 18 and Figure 23. Steel mechanical properties defined for this part.

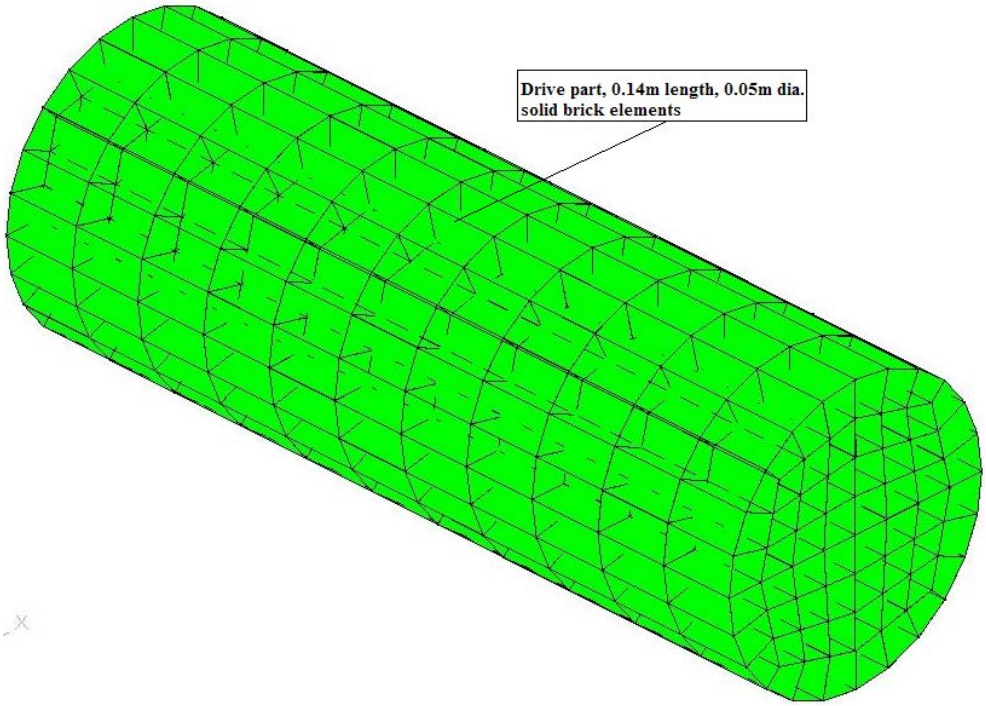

Figure 22: Drive part of the characteristic model

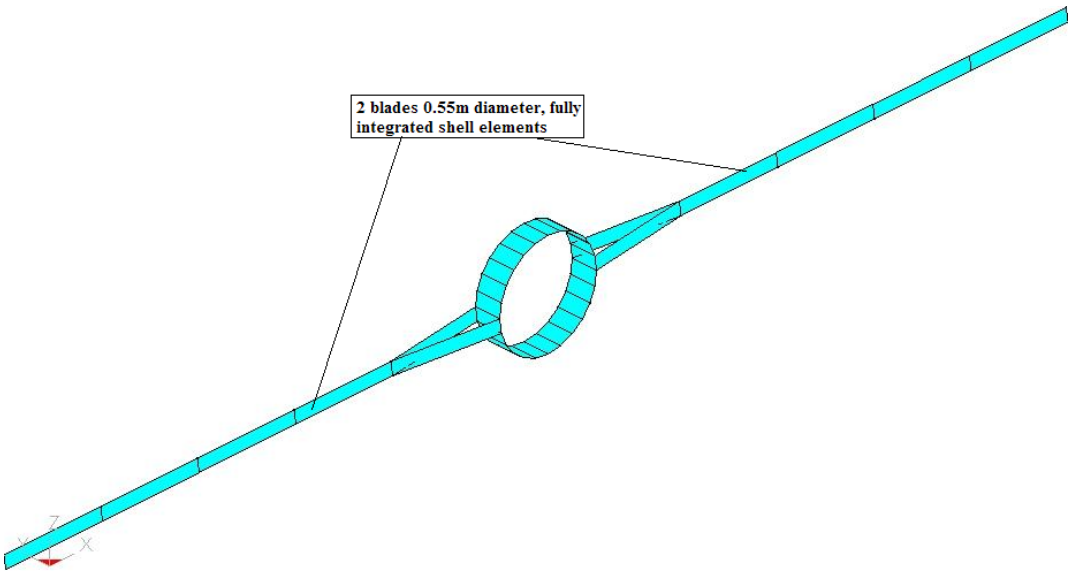

Figure 23: Blades part of the characteristic model

3.9 Seabed Part of the Characteristic Model

Defined to simulate seabed modelled with fully integrated shells (type 16) and rigid material as required by the finite rigid wall contact condition given to this part. The location of this part shown in Figure 11 and Figure 12 while the geometry of (1.12mx1.12mx0.002m) shown in Figure 24. The assumed mechanical properties are those of the soil mechanics.

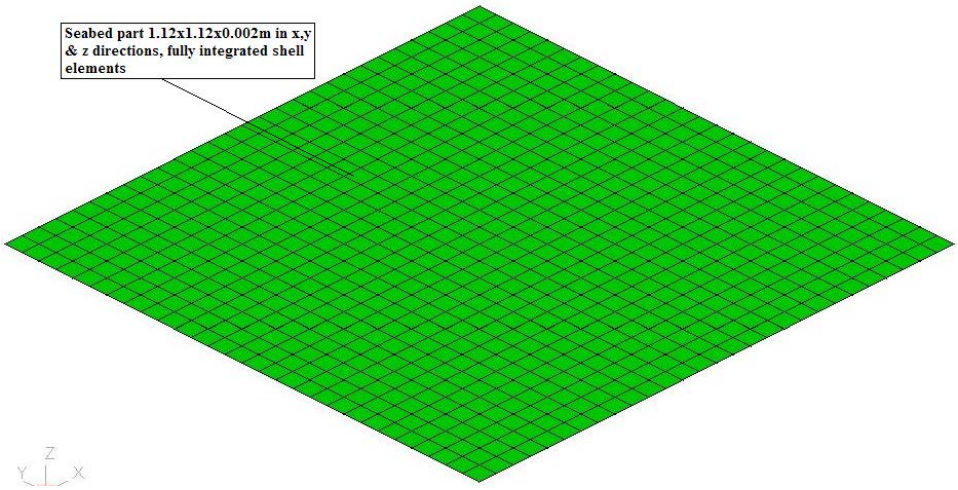

Figure 24: Seabed part of the characteristic model

4. Analysis of the Characteristic Model

The material cards, property cards, control cards, constraints and boundaries, References [4,5,6,7,8] are employed here. Gravity force first applied ramped over a short time, while characteristic forces simulating the effects of hydrodynamic forces on the floating support side, aerodynamic forces on the blades and upwind pressure on nacelle upwind face all applied ramped after full gravity was in action over a short time as well. This aimed at allowing enough time for gravity forces to generate the required pressure and avoiding spurious dynamic effects in the system. Unfortunately, because of the conditional stability of the explicit finite element analysis there is no 'quick' solution to the long time required for the analysis. The time step size has to be smaller than a critical value. This critical value is directly dependent on the largest frequency of the finite element discretization (smallest element). Consequently, in larger scale problems the time step becomes extremely short (10^{-7} sec) in this case, with all negative effects on the computer run time and possibly memory as well. In order for the buoyancy pressure to build up in the (ALE) water elements longer time needed for body load application to achieve this. Different parts of this model created in consecutive order starting with the rigid wall representing the seabed, the two ALE parts and the floating support. Then the model run and the next top parts added one at a time and run to assure the desired behaviour. Due to problems introduced by modelling the cable the results shown hereafter are for the float only with other parts excluded. These model verification results are as follows:

The displaced volume = $(0.4)^3 + (0.64)^2 \times 0.2 = 0.1459$ m^3 and uplift buoyancy force is:

$F_{buoyancy} = 0.1459 \times 1025 \times 9.81 = 1467.26$ N,

The force at the bottom face of the hull is:

$1467.26 + 0.472 \times 1025 \times 9.81 \times (0.64)^2 = 3411.25$ N, this is conforming to the code calculated z-force shown in Figure 25.

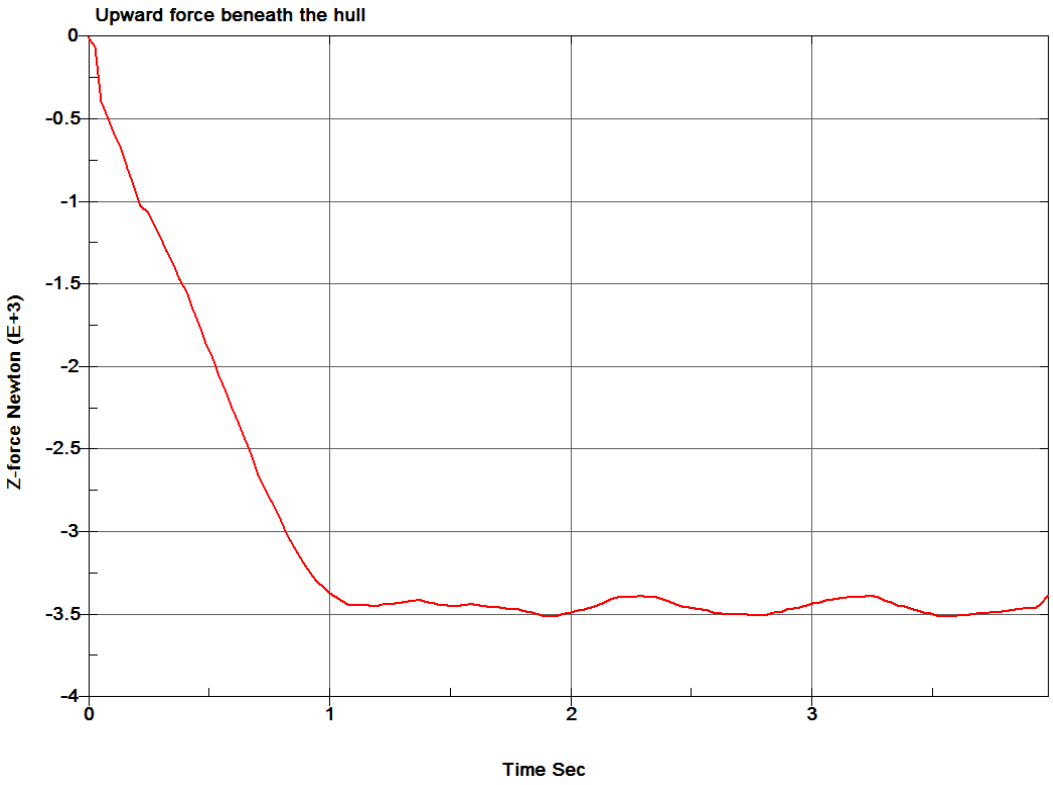

Figure 25: Uplift force on the floating support bottom

Meanwhile z-direction stress under the floating support calculated as follows:

$\sigma_{zz} = \frac{3411.25}{0.64 \times 0.64} =$ 8328.25 Pa, this value is close enough to the code calculated value shown in Figure 26.

Moreover, for base side element of the floating support, the water pressure due to vertical position of this element centre of 0.60m is:

P_{xx} =0.60 x 1025 x 9.81 = 6033 Pa this in close agreement with the calculated pressure value for the same element shown in Figure 27.

In the same sequence picking up an element at the edge of the floating support base, the forces calculated at the two edge nodes of the element is (-5.8 N) while those at the two top edge of the same element is (-6.6 N) as calculated by the LS-DYNA3D code. Therefore, this element share of these forces is (-2 x 5.8 /2 + (-6.6) x 2/4) = - 9.1N this is translated to an element stress in x-direction = $\frac{9.1}{0.04 \times 0.04}$ = - 5688 Pa which is close to the value shown in Figure 28.

The hull kinetic energy as shown in Figure 29 is well within the converged stable system with dying kinetic energy.

It is worth noting that the smoothness of the above curves attributed to a higher damping applied for the floating hull run of the characteristic model.

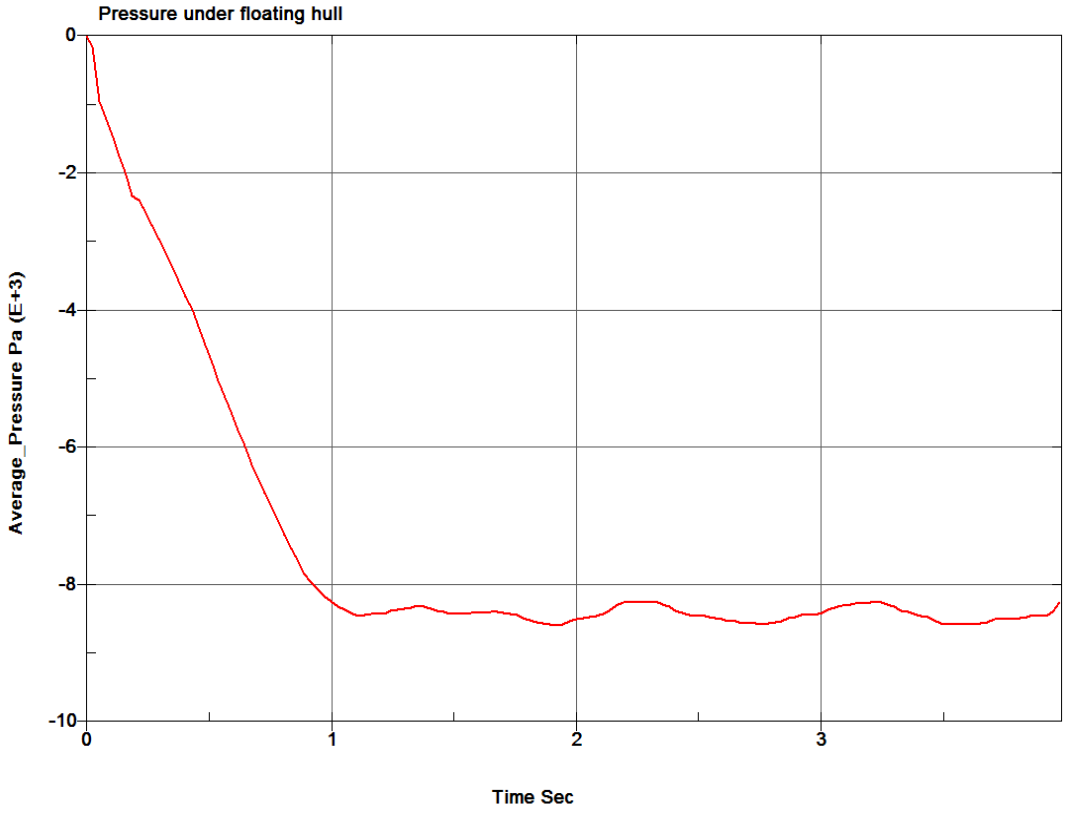

Figure 26: Pressure on the bottom face of the hull support

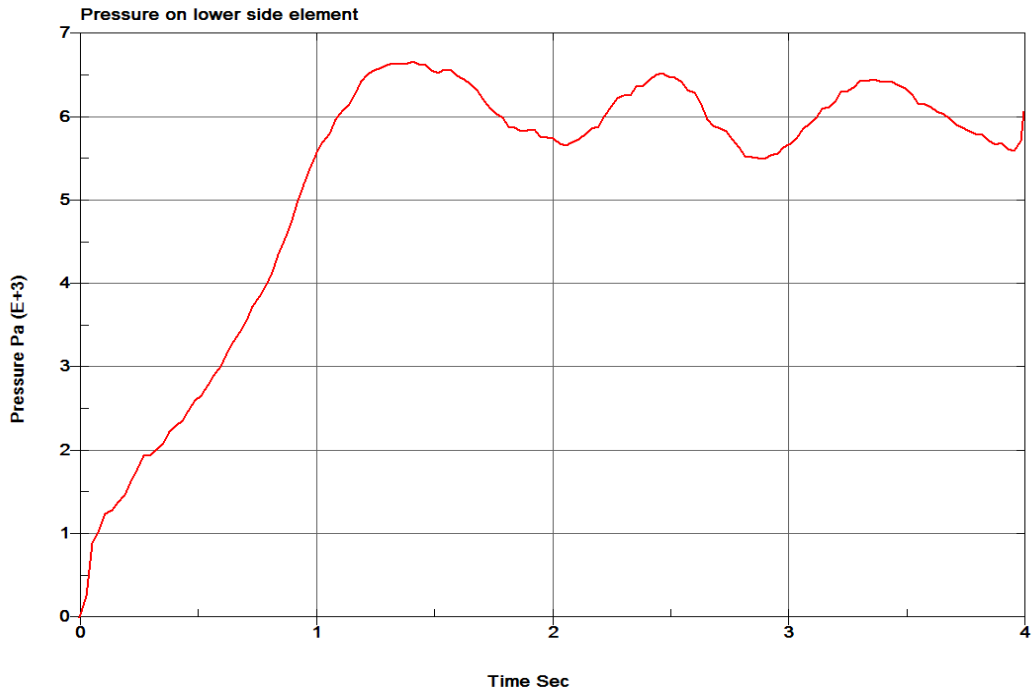

Figure 27: Pressure on bottom side element of the hull support

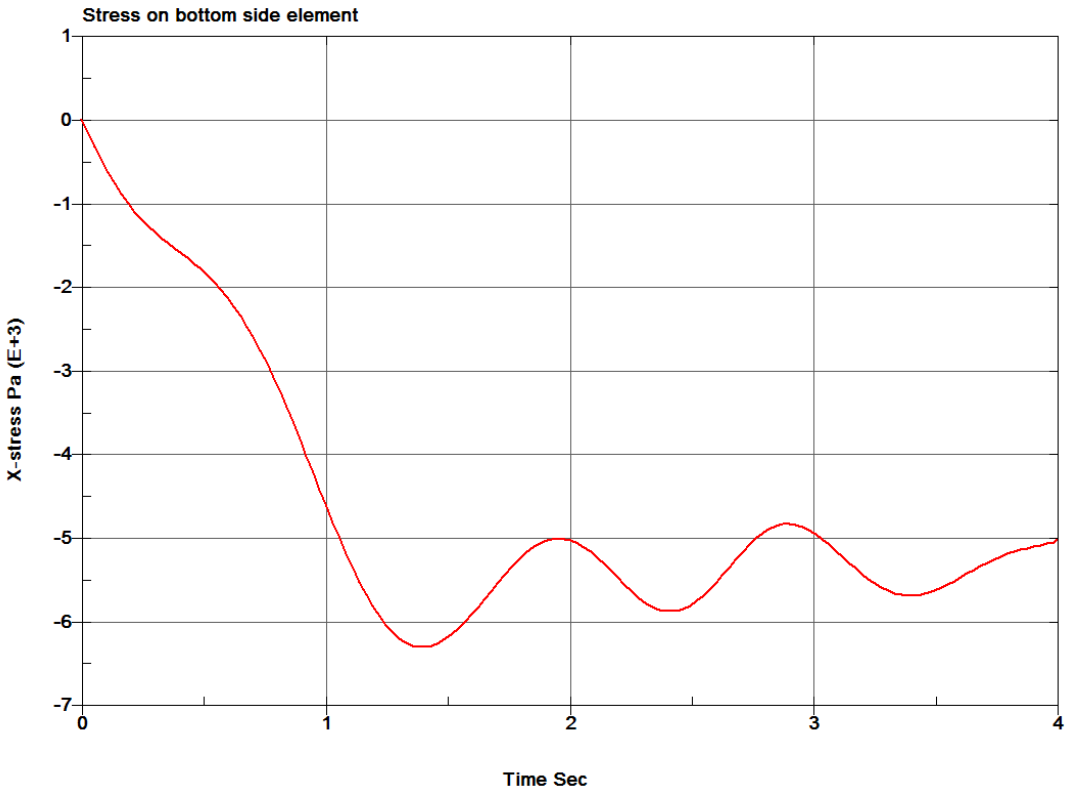

Figure 28: Stress on the base element face of the support hull

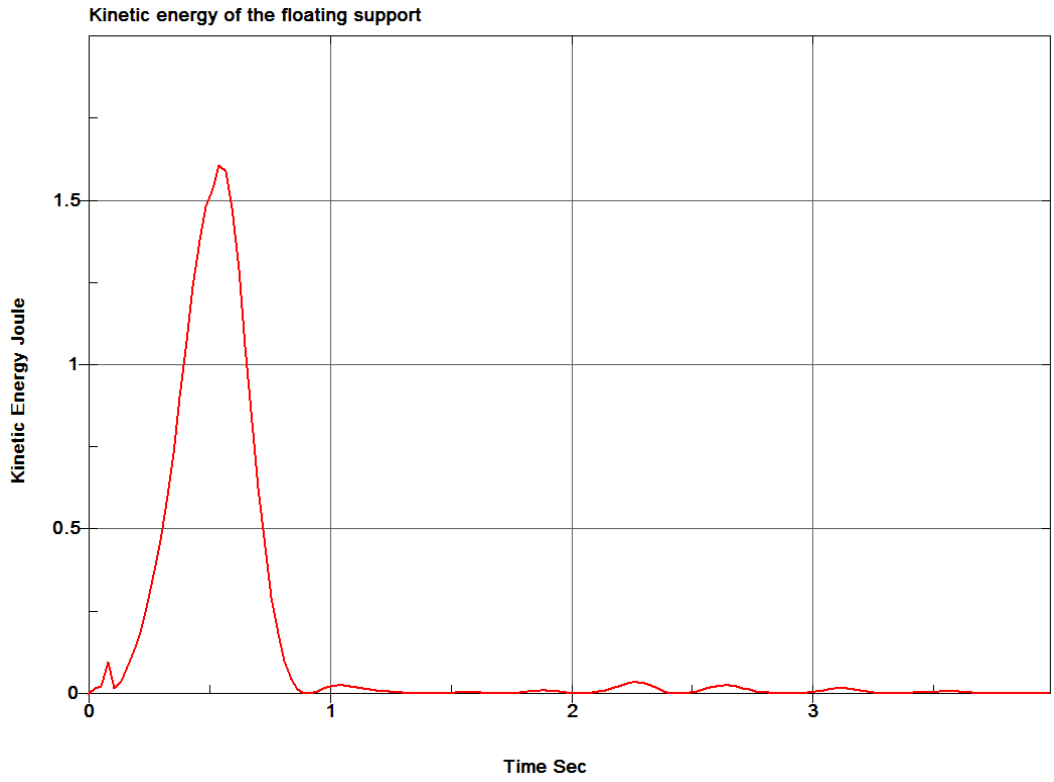

Figure 29: Kinetic energy for floating support hull

5. Discussions of the Verification Model

5.1 General

This paper has demonstrated that there are a number of options and issues considered for the validation/verification of finite element techniques applicable for modelling an offshore floating wind energy converter.

5.2 ALE

The results for simple three-dimensional float model utilizing the ALE formulation yield believable results under normal gravity loading, both through visual inspection and comparison of buoyancy states and pressures on the float body with that derived from hand calculation.

All loading was ramped from zero over what was judged as a suitable (and feasible in terms of analysis runtime) time scale. The float was seen to 'bob' vertically in the water with its amplitude of motion decreasing with time, therefore it was judged that any effects from the short ramping duration of loading to its full value causing a 'pseudo-impact' are negligible if the model is given enough time for the kinetic energy to dissipate. The two-dimensional finite element modelling has studied buoyancy effects and it concluded that LS-DYNA3D models this correctly. Different states of stability and angles of list are comparable with hand calculation predictions and engineering judgement based on prior knowledge of rigid blocks on very flexible foundations gives confidence in the model behaviour.

The application of transverse loading caused the float to rotate and sink as expected, though no comparisons made with hand calculations for this load case. Based on these observations the judgement that the ALE formulation would be suitable as modelled and applicable for incorporation in a detailed model.

5.3 Turbine Model

The tower, turbine rotor blades, nacelle (with associated inside parts) and bearings are all relatively straightforward parts to model in terms of achieving the appropriate coupling and desired behaviour. The rotor blades seen to turn and the nacelle rotates in plan under appropriate load regimes, and there is therefore a high degree of confidence that these parts will perform as expected.

5.4 Mooring Cables

In reality, the polyester cables anchored to the seabed and pass through a slip ring mounted on the side of the concrete hull and the cable ultimately fixed near the top of the hull. Hence, the cable can effectively slide through the slip ring. As a simplified logical representation, ordinary beam elements with tension only formulation were employed. Again, logically these beam elements coupled to the body of the water so that they could interact with the water, as they would do in reality.

Many problems faced in modelling the cables due to contact and coupling problems with the ALE. Different approaches adopted such as replacing the tension only 'cable' elements with 'seatbelt' representations, and applying pre-tension to the cables. However, the results all showed problems of sinking or breakdown of the cable representation at the air/water interface. Some of the problems faced been alleviated, but the solution run times involved have meant that there are no meaningful results currently available in terms of cable anchorage forces.

There are a number of issues surrounding the modelling of cable and membrane structures, which theoretically carry only tensile forces. Cook and his colleagues [9] highlights some of these issues, which relate to the absence of flexural stiffness and subsequent large deflections. In some instances, these problems may lead to convergence difficulties, which overcome by adding some small flexural stiffness, i.e. produce along very flexible beam element.

5.5 Boundary Conditions

Aside from the coupling and constraints for the nacelle, bearing, and rotor blades, the other important boundary is that which surrounds the water. A suitable size for the body of the water selected appropriately to model the semi-infinite space. Guidelines exist on modelling 'half-spaces' in finite element models when dealing with soil in soil-structure interaction problems, but for now the size of the water was modelled as a conservatively large enough body to capture interaction effects. To dissipate the energy of the wave and water motion from the model, energy-absorbing (non-reflecting) boundaries employed.

Some of the time-history stress plots initially showed some 'noise' before filtering applied. Analysis using the 'Fast Fourier Transform' approach was inconclusive, though two areas of which may be sourcing the noise identified. Internal reflection from boundaries cannot ruled out, and the more likely cause is that of chattering of the fluid-structure coupling. In either case, filtering appears to remove the noise and the results appear to be as expected when compared with hand-calculated values, therefore it concluded that the noise has little effect on the action of the model.

6. Conclusions

As a general conclusion, there is a high degree of confidence that the majority of the modelling techniques investigated in this validation and verification process employed in a detailed characteristic structure in severe environmental loads. The main area for concern is that for the cables as these provide the all-important anchoring forces, which will affect the forces generated in the floating structure. Powerful features employed showed good agreement in modelling.

7. Recommendations and future work

A characteristic modelling work carried out and its objective was to show the excellent capabilities of the explicit LSDYNA3D code in modelling complex structure in hostile loadings. The aim was to push the finite element analysis to its limit so the latest techniques investigated and employed, however, this highlighted

potential problems both in complexity, formulation difficulties in some aspects of the modelling and the level of detail adopted. The efforts in building a characteristic model showed good results in terms of code capabilities in modelling a complicated structure in harsh environment. Furthermore, a 'detailed' full-scale model need to be constructed and subject to analysis runs under straightforward load cases such as gravity and transverse wind, buoyancy and wave loading.

A considerable degree of debugging results once the model run for analysis. Strongly recommended for future work: further debugging significantly required using another parallel strong finite element code such as ABAQUS employing up to date loading and boundary conditions for this structure. The fatigue problem, expected to be the main concern for such structure, therefore further future work should focus on this mode of failure as well.

8. List of Figures

References

[1] Mohamed A Almherigh, “Evaluation of Finite Element Techniques Applied to Floating Offshore Wind Turbine” Ph. D thesis, The University of Salford, Salford, UK, 2006.

[2] Vugts J h et al “Design of the Support Structure of an Optimised Offshore Wind Energy Converter”

[3] Henderson A R et al “Prospects for Floating Offshore Wind Energy” European Wind Energy Conference, Copenhagen, 2–6 July 2001.

[4] LSTC “LS-DYNA Keyword User’s Manual Volume II (Material Models, References and Application)”

March 2001, version 960 Livermore Software Technology Corporation, PDF file online, LSTC website. http://www.lstc.com/, January 2003.

[5] LSTC "LSPOST A New Post Processor For LSDYNA", May 1999, Livermore Software Technology Corporation, PDF online file, LSTC website. http://www.lstc.com/ , April 2003.

[6] LSTC "LS-DYNA Keywords User's Manual" April 2003, Version 970 Livermore Technology Corporation, PDF online, LSTC website. http://www.lstc.com/ , July 2003.

[7] LSTC "LS-DYNA Keywords User's Manual" April 2003, Version 970 Livermore Technology Corporation, PDF online, LSTC website. http://www.lstc.com/ , July 2003.

[8] LSTC "LS-DYNA Keyword User's Manual Volume II (Material Models, References and Application)" March 2001, version 960 Livermore Software Technology Corporation, PDF file online, LSTC website. http://www.lstc.com/ , January 2003.

[9] R D Coock et al "Concepts and Applications of Finite Element Analysis" John Wiley & Sons 2002. Proc. EWEC' 99 (1999).